IX-E Biomolecular Science

Elucidation of a structure-function relationship of metalloproteins and structural chemistry of amyloid are current subjects of this group. The primary technique used for the first project is the stationary and time-resolved resonance Raman spectroscopy excited by visible and UV lasers. IR-microscope dichroism analysis and AFM are the main techniques for the second project. The practical themes that we want to explore for the first project are (1) mechanism of oxygen activation by enzymes, (2) mechanism of active proton translocation and its coupling with electron transfer, (3) structural mechanism of signal sensing and transduction by heme-based sensor proteins, (4) higher order protein structures and their dynamics, and (5) reactions of biological NO. In category (1), we have examined a variety of terminal oxidases, cytochrome P450s, and peroxidases, and also treated their enzymatic reaction intermediates by using the mixed flow transient Raman apparatus and the Raman/absorption simultaneous measurement device. For (2) the third-generation UV resonance Raman (UVRR) spectrometer was constructed and we are going to apply it to a giant protein like cytochrome *c* oxidase. Recently, we succeeded in pursuing protein folding of apomyoglobin by combining UV time-resolved Raman and rapid mixing device. We also determined the carboxylic side chains of bovine cytochrome oxidase which undergo protonation/deprotonation changes and hydrogen-bonding status changes in response with electron transfers between metal centers or ligand dissociation from heme a_3. Currently, we focus our attention on detecting tyrosine radical for the P intermediate of terminal oxidases. Some positive evidence was obtained for cytochrome *bo*. In (3) we are interested in a mechanism of ligand recognition specific to CO, NO or O_2 and communication pathway of the ligand binding information to the functional part of the protein. For (4) we developed a novel technique for UV resonance Raman measuremnts based on the combination of the first/second order dispersions of gratings and applied it successfully to 235-nm excited RR spectra of several proteins including mutant hemoglobins and myoglobins. Nowadays we can carry out time-resolved UVRR experiments with nanosecond resolution to discuss protein dynamics. With the newly developed third generation UV Raman spectrometer, we have succeeded in isolating the spectrum of tyrosinate in ferric Hb M Iwate, which was protonated in the ferrous state, and the deprotonated state of Tyr244 of bovine cytochrome *c* oxidase. As a model of Tyr244, an imidazole-bound *para*-cresol was synthesized and its UV resonance Raman was investigated. For (5) we purified soluble guanylate cyclase from bovine lung and observed its RR spectra. To further investigate it, we are developing an expression system of this protein. For the amyloid study, we examined FTIR spectra of β_2-microglobulin and its #11-21 peptides which form a core part of amyloid fibril.

IX-E-1 FTIR Detection of Protonation/Deprotonation of Key Carboxyl Side Chains Caused by Redox Change of the Cu_A-Heme *a* Moiety and Ligand Dissociation from the Heme a_3-Cu_B Center of Bovine Heart Cytochrome *c* Oxidase

OKUNO, Daichi[1]; IWASE, Tadashi; SHINZAWA-ITOH, Kyoko[2]; YOSHIKAWA, Shinya[2]; KITAGAWA, Teizo
([1]GUAS; [2]Himeji Inst. Tech.)

[*J. Am. Chem. Soc.* **125**, 7209–7218 (2003)]

FTIR spectral changes of bovine cytochrome *c* oxidase (CcO) upon ligand dissociation from heme a_3 and redox change of the Cu_A-heme *a* moiety (Cu_AFe_a) were investigated. In a photosteady state under CW laser illumination at 590 nm to carbonmonoxy CcO (CcO–CO), the C–O stretching bands due to $Fe_{a3}^{2+}CO$ and $Cu_B^{1+}CO$ were identified at 1963 and 2063 cm^{-1}, respectively, for the fully reduced (FR) state [$(Cu_AFe_a)^{3+}Fe_{a3}^{2+}Cu_B^{1+}$] and at 1965 and 2061 cm^{-1} for the mixed valence (MV) state [$(Cu_AFe_a)^{5+}Fe_{a3}^{2+}$-$Cu_B^{1+}$] in H_2O as well as in D_2O. For the MV state, however, another band due to $Cu_B^{1+}CO$ was found at 2040 cm^{-1}, which was distinct from the α/β conformers in the spectral behaviors, and therefore was assigned to the $(Cu_AFe_a)^{4+}Fe_{a3}^{3+}Cu_B^{1+}CO$ generated by back electron transfer. The FR-minus-oxidized difference spectrum in the carboxyl stretching region provided two negative bands at 1749 and 1737 cm^{-1} in H_2O, which were apparently merged into a single band with a band center at 1741 cm^{-1} in D_2O. Comparison of these spectra with those of bacterial enzymes suggests that the 1749 and 1737 cm^{-1} bands are due to COOH groups of Glu242 and Asp51, respectively. A similar difference spectrum of the carboxyl stretching region was also obtained between $(Cu_AFe_a)^{3+}Fe_{a3}^{2+}Cu_B^{1+}CO$ and $(Cu_AFe_a)^{5+}Fe_{a3}^{2+}Cu_B^{1+}CO$. The results indicate that an oxidation state of the (Cu_AFe_a) moiety determines the carboxyl stretching spectra. On the other hand, CO-dissociated minus CO-bound difference spectra in the FR state gave rise to a positive and a negative peaks at 1749 and 1741 cm^{-1}, respectively, in H_2O, but mainly a negative peak at 1735 cm^{-1} in D_2O. It was confirmed that the absence of a positive peak is not caused by slow deuteration of protein. The corresponding difference spectrum in the MV state showed a significantly weaker positive peak at 1749 cm^{-1} and an intense negative peak at 1741 cm^{-1} (1737 cm^{-1} in D_2O). The spectral difference between the FR and MV states is explained satisfactorily by the spectral change induced by the electron back flow upon CO dissociation as described above. Thus, the changes of carboxyl stretching bands induced both by oxidation of (Cu_AFe_a) and dissociation of CO appear at similar frequencies (~ 1749 cm^{-1}) but are ascribed to different carboxyl side chains.

IX-E-2 Core Structure of Amyloid Fibril Proposed from IR-Microscope Linear Dichroism

HIRAMATSU, Hirotsugu; GOTO, Yuji[1]; NAIKI,

Hironobu[2]; KITAGAWA, Teizo
([1]Osaka Univ.; [2]Fukui Medical Univ.)

[*J. Am. Chem. Soc.* submitted (2003)]

A new approach for studying a peptide conformation of amyloid fibril has been developed. It is based on infrared linear dichroism analysis using an IR-microscope for aligned amyloid fibril. The polarization directions of amide I and II bands were perpendicular similarly for β_2-microglobulin and its #21-31 peptide. Furthermore, this approach has shown that the #21-31 peptide consists of two C=O bonds in the β-sheet that makes 0° with the fibril axis, three C=O bonds in the β-sheet inclined by 27° with respect to the fibril axis, four residues in the random coil by 47°, and two residues in possible β-bulge structure by 32°. Plausible structures of the amyloid core in the fibril is proposed by taking account of these results.

IX-E-3 Resonance Raman Characterization of the P Intermediate in the Reaction of Bovine Cytochrome *c* Oxidase

OGURA, Takeshi[1]; KITAGAWA, Teizo
([1]Himeji Inst. Tech.)

[*Biochim. Biophys. Acta* in press (2003)]

Reduced cytochrome *c* oxidase binds molecular oxygen, yielding an oxygenated intermediate first (Oxy) and then converts it to water *via* the reaction intermediates of P, F, and O in the order of appearance. We have determined the iron-oxygen stretching frequencies for all the intermediates by using time-resolved resonance Raman spectroscopy. The bound dioxygen in Oxy does not form a bridged structure with Cu_B and the rate of the reaction from Oxy to P (P_R) is slower at higher pH in the pH range between 6.8 and 8.0. It was established that the P intermediate has an oxo-heme and definitely not the Fe_{a3}–O–O–Cu_B peroxy bridged structure. The Fe_{a3}=O stretching ($\nu_{Fe=O}$) frequency of the P_R intermediate, 804/764 cm^{-1} for $^{16}O/^{18}O$, is distinctly higher than that of F intermediate, 785/750 cm^{-1}. The rate of reaction from P to F in D_2O solution is evidently slower than that in H_2O solution, implicating the coupling of the electron transfer with vector proton transfer in this process. The P intermediate (607 nm form) generated in the reaction of oxidized enzyme with H_2O_2 gave the $\nu_{Fe=O}$ band at 803/769 cm^{-1} for $H_2{}^{16}O_2$/$H_2{}^{18}O_2$ and the simultaneously measured absorption spectrum exhibited the difference peak at 607 nm. Reaction of the mixed valence CO adduct with O_2 provided the P intermediate (P_M) giving rise to an absorption peak at 607 nm and the $\nu_{Fe=O}$ bands at 804/768 cm^{-1}. Thus, three kinds of P intermediates are considered to have the same oxo-heme a_3 structure. The ν_4 and ν_2 modes of heme a_3 of the P intermediate were identified at 1377 and 1591 cm^{-1}, respectively. The Raman excitation profiles of the $\nu_{Fe=O}$ bands were different between P and F. These observations may mean the formation of a π cation radical of porphyrin macrocycle in P.

IX-E-4 Heme Strctures of Five Hemoglobin Ms Probed by Resonance Raman Spectroscopy

JIN, Yayoi[1]; NAGAI, Masako[1]; NAGAI, Yukifumi[1]; NAGATOMO, Shigenori; KITAGAWA, Teizo
([1]Kanazawa Univ.)

[*Biochemmistry* submitted (2003)]

The α-abnormal Hb Ms show physiological properties different from the β-abnormal Hb Ms, that is, extremely low oxygen affinity of the normal subunit and extraordinary resistance to both enzymatic and chemical reduction of the abnormal met-subunit. In order to get insight into contribution of the heme structure to these differences among Hb Ms, we examined the 406.7-nm excited resonance Raman (RR) spectra of five Hb Ms in the frequency region from 1700 to 200 cm^{-1}, which afford some essential information on the heme structure. The spectra of the abnormal met-subunit in the high frequency region were extracted by the difference calculations between the spectra of the fully-met Hb Ms and of metHb A to eliminate overlaps of the RR bands of the fully-met Hb Ms with those of normal met-subunits. For the half-met Hb Ms (abnormal subunits in the met-form and normal subunits in the deoxy-form), RR bands due to abnormal met-subunits could be clearly distinguished from those of normal deoxy-subunits except for ν_7. In the high frequency region, profound differences between met-α abnormal subunits and met-β abnormal subunits were observed for the in-plane skeletal mode (the $\nu_{C=C}$, ν_{37}, ν_2, ν_{11} and ν_{38} bands), probably reflecting different distortion of the heme structure by the displacement of the heme iron due to tyrosine coordination. Below 900 cm^{-1}, Hb M Iwate (αF8-Tyr) exhibited a distinct spectral pattern for ν_{15}, γ_{11}, $\delta(C_bC_aC_b)_{2,4}$, and $\delta(C_bC_cC_d)_{6,7}$ compared to that of Hb M Boston (αE7-Tyr), although both heme irons are coordinated by Tyr. The β-abnormal Hb Ms, namely, Hb M Hyde Park (βF8-Tyr), Hb M Saskatoon (βE7-Tyr) and Hb M Milwaukee (βE11-Glu), displayed RR band patterns similar to that of metHb A, but with some minor individual differences. The RR bands characteristic of the met-subunits of Hb Ms totally disappeared by chemical reduction and the ferrous heme of abnormal subunits was no more bonded with Tyr or Glu. They were bound to the distal (E7) or proximal (F8) His, and this was confirmed by the presence of the $\nu_{Fe–His}$ mode at 215 cm^{-1} in the 441.6-nm excited RR spectra. A possible involvement of heme distortion in differences of reducibility of abnormal subunits and oxygen affinity of normal subunits is discussed.

IX-E-5 Heme-Regulated Eukaryotic Initiation Factor 2a Kinase (HRI) Activation by Nitric Oxide Is Induced by Formation of Five-Coordinated NO-Heme Complex: Optical Absorption, Electron Spin Resonance and Resonance Raman Spectral Studies

IGARASHI, Jotaro[1]; SATO, Akira; KITAGAWA, Teizo; YOSHIMURA, Tetsuhiko[2]; YAMAUCHI, Seigo[1]; SAGAMI, Ikuko[1]; SHIMIZU, Toru[1]
([1]Tohoku Univ.; [2]Yamagata Public Co. Develop. Ind.)

[*J. Biol. Chem.* submitted (2003)]

Heme-regulated eukaryotic initiation factor 2a (eIF2a) kinase (HRI) regulates the synthesis of hemoglobin in reticulocytes in response to heme availability. HRI has tightly bound heme at the N-terminal domain. Nitric oxide (NO) has been reported to regulate HRI catalysis, but its mechanism remains unclear. In the present study, we examined *in vitro* kinase assay, optical absorption, electron spin resonance (ESR) and resonance Raman spectra of full-length HRI to elucidate regulation mechanism by NO. HRI was activated *via* heme upon NO binding and the Fe(II)HRI(NO) complex had 5-fold eIF2a kinase activity compared to the Fe(III)HRI complex. The Fe(III)HRI complex had Soret peak at 415 nm and exhibited a rhombic ESR signal with *g* values of 2.49, 2.28 and 1.87, suggesting that the Fe(III)HRI complex would be coordinated with His and Cys as axial ligands. Upon addition of NO to the Fe(II)HRI complex, the Soret peak shifted from 423 nm to 398 nm, indicating formation of 5-coordinate NO-heme complex. ESR spectra of the Fe(II)HRI(NO) complex showed a hyperfine triplet, characteristic of 5-coordinate NO-heme complex. Resonance Raman studies showed that Fe–NO and N–O stretching frequencies were located at 527 and 1677 cm^{-1}, respectively in the Fe(II)HRI(NO) complex and that Fe–His stretching frequency was observed at 219 cm^{-1}, immediately after photolysis from the Fe(II)HRI(CO) complex. The spectral findings obtained with full-length HRI were totally different from those obtained with the isolated N-terminal heme-binding domain. We will discuss roles of NO and heme in catalysis with HRI, taking account of heme-based sensor proteins.

IX-E-6 Structural and Spectroscopic Features of a *cis* (Hydroxo)-Fe^{III}-(Carboxylato) Configuration as an Active Site Model for Lipoxygenases

OGO, Seiji[1]; YAMAHARA, Ryo[2]; ROACH, Mark; SUENOBU, Tomoyoshi[3]; AKI, Michihiko; OGURA, Takashi[4]; KITAGAWA, Teizo; MASUDA, Hideki[5]; FUKUZUMI, Shunichi[3]; WATANABE, Yoshihito[6]
([1]IMS and Osaka Univ.; [2]Osaka Univ. and Nagoya Inst. Tech.; [3]Osaka Univ.; [4]Univ. Tokyo; [5]Nagoya Inst. Tech.; [6]Nagoya Univ.)

[*Inorg. Chem.* **41**, 5513–5520 (2002)]

In our preliminary communication (Ogo, S.; Wada, S.; Watanabe, Y.; Iwase, M.; Wada, A.; Harata, M.; Jitsukawa, K.; Masuda, H.; Einaga, H. *Angew. Chem., Int. Ed.* **37**, 2102–2104 (1998)), we reported the first example of X-ray analysis of a mononuclear six-coordinate (hydroxo)iron(III) non-heme complex, $[Fe^{III}(tnpa)(OH)(RCO_2)]ClO_4$ [tnpa = tris(6-neopentylamino-2-pyridylmethyl)amine; for **1**, R = C_6H_5], which has a characteristic *cis* (hydroxo)-Fe^{III}-(carboxylato) configuration that models the *cis* (hydroxo)-Fe^{III}-(carboxylato) moiety of the proposed (hydroxo)iron(III) species of lipoxygenases. In this full account, we report structural and spectroscopic characterization of the *cis* (hydroxo)-Fe^{III}-(carboxylato) configuration by extending the model complexes from **1** to $[Fe^{III}(tnpa)(OH)(RCO_2)]ClO_4$ (**2**, R = CH_3; **3**, R = H) whose *cis* (hydroxo)-Fe^{III}-(carboxylato) moieties are isotopically labeled by $^{18}OH^-$, $^{16}OD^-$, $^{18}OD^-$, $^{12}CH_3{}^{12}C^{18}O_2^-$, $^{12}CH_3{}^{13}C^{16}O_2^-$, $^{13}CH_3{}^{12}C^{16}O_2^-$, $^{13}CH_3{}^{13}C^{16}O_2^-$, and $H^{13}C^{16}O_2^-$. Complexes **1**–**3** are characterized by X-ray analysis, IR, EPR, and UV-vis spectroscopy, and electrospray ionization mass spectrometry (ESI-MS).

IX-E-7 Low-Temperature Stopped-Flow Studies on the Reactions of Copper(II) Complexes and H_2O_2: The First Detection of a Mononuclear Copper(II)-Peroxo Intermediate

OSAKO, Takao[1]; NAGATOMO, Shigenori; TACHI, Yoshimitsu[1]; KITAGAWA, Teizo; ITOH, Shinobu[1]
([1]Osaka City Univ.)

[*Angew. Chem., Int. Ed.* **41**, 4325–4328 (2002)]

Mononuclear copper-active oxygen complexes are key reactive intermediates in many biological and catalytic oxidation processes, but no information is presently available from model systems about mononuclear Cu^{II}-peroxo species. Herein, low-temperature stopped-flow studies are described for the reactions of copper(II) complexes supported by tridentate ligands (L1 and L2) with H_2O_2 to demonstrate that a mononuclear Cu^{II}-peroxo complex is generated from an initially formed Cu^{II}-hydroperoxo intermediate [Equations. (2) and (3)]. The results represent the first example of the direct detection of a mononuclear Cu^{II}-peroxo complex, which provides important information about the reactive intermediates involved in biological and industrial oxidation processes.

$$H_2O_2 + Et_3N \underset{}{\overset{K_1}{\rightleftharpoons}} HO_2^- Et_3NH^+ \quad (1)$$

$$[LCu^{II}]^{2+} + HO_2^- Et_3NH^+ \xrightarrow{k_1} [LCu^{II}\text{-}OOH] + Et_3NH^+ \quad (2)$$
(A)

$$LCu^{II}\text{-}OOH \xrightarrow{k_2} LCu^{II}(O_2) \xrightarrow{k_3[Cu^{II}(L)]} LCu^{II}(O_2)Cu^{II}L \quad (3)$$
(A) (B) (C)

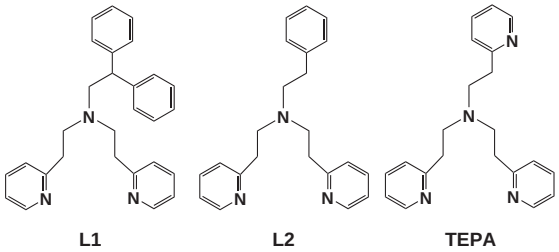

Figure 1.

IX-E-8 Ligand Effect on Reversible Conversion between Copper(I) and Bis(μ-oxo)Dicopper(III) Complex with a Sterically Hindered Tetradentate Tripodal Ligand and Monooxygenae Activity of Bis(μ-oxo)Dicopper(III) Complex

MIZUNO, Masayasu[1]; HAYASHI, Hideki[1];

FUJINAMI, Shuhei[1]; NAGATOMO, Shigenori; OTAKE, Shigenori[1]; UOZUMI, Kounosuke[1]; SUZUKI, Masatatsu[1]; KITAGAWA, Teizo
([1]Kanazawa Univ.)

[*Inorg. Chem.* submitted (2003)]

A new sterically hindered tetradentate tripodal ligand (Me_2-etpy) and its deuterated ligand of the methylene hydrogens (d_4-Me_2-etpy) were synthesized, where Me_2-etpy is bis(6-methyl-2-pyridylmethyl)(2-pyridylethyl)amine. Copper(I) complexes $[Cu(Me_2\text{-etpy}$ or $d_4\text{-}Me_2\text{-etpy})]^+$ (**1** and **1**-d_4, respectively) reacted with dioxygen at –80 °C in acetone to give bis(μ-oxo)dicopper(III) complexes $[Cu_2(O)_2(Me_2\text{-etpy}$ or $d_4\text{-}Me_2\text{-etpy})_2]^{2+}$ (**1**-oxo and **1**-d_4-oxo respectively), the latter of which was crystallographically characterized. Unlike a bis(μ-oxo)dicopper(III) complex with a closely related Me_2-tpa ligand having a 2-pyridylmethyl pendant, **1**-oxo possessing a 2-pyridylethyl pendant is not fully formed even under 1 atm of O_2 at –80 °C and is very reactive toward the oxidation of the supporting ligand. **1**-oxo has a regioselective monooxygenase activity toward the methylene group of the supporting ligand to give a *N*-dealkylated ligand in yield ~ 80% based on a dimer and a corresponding aldehyde. The deuterated ligand d_4-Me_2-etpy greatly stabilizes the bis(μ-oxo)dicopper(III) complex **1**-d_4-oxo, indicating that the rate determining step of the *N*-dealkylation is the hydrogen abstraction from the methylene group. The reversible conversion between **1**-d_4 and **1**-d_4-oxo in acetone was observed depending on the temperature and the thermodynamic parameters (ΔH and ΔS) of the equlibrium were determined to be -53 ± 2 kJ mol^{-1} and -187 ± 10 J mol^{-1}K^{-1}, respectively. The effect of the 2-pyridylethyl pendant in comparison with the 2-pyridylmethyl and 6-methyl-2-pyridylmethyl pendants on the physicochemical properties of the copper(I) and bis(μ-oxo)dicopper(III) species is discussed. (X-ray crystallography (Crystal data for **1**·ClO_4: monoclinic, *C2/c*, a = 20.305(4) Å, b = 12.705(2) Å, c = 16.867(3) Å, β = 100.123(4) Å, V = 4283(1) Å^3, Z = 8, R = 0.044 and R_W = 0.064 ($I \geq 0.0\sigma(\boldsymbol{I})$); for **1**-$d_4$-oxo·$ClO_4$: triclinic, *P*1, a = 10.910(4) Å, b = 11.259(4) Å, c = 14.986(5) Å, α = 82.38(2)°, β = 71.48(2)°, γ = 84.69(2)°, V = 1727(1) Å^3, Z = 1, R = 0.118 and R_W = 0.123($I \geq 0.0\sigma(\boldsymbol{I})$); for **1**-OMe·$ClO_4$: monoclinic, $P2_1/c$, a = 11.642(3) Å, b = 16.689(4) Å, c = 12.885(4) Å, β = 97.700(6)°, V = 2480(1) Å^3, Z = 2, R = 0.031 and R_W = 0.040($\boldsymbol{I} \geq 3\sigma(\boldsymbol{I})$)).

IX-E-9 Dinuclear Copper-Dioxygen Intermediates Supported by Polyamine Ligands

TERAMAE, Shinichi[1]; OSAKO, Takao[2]; NAGATOMO, Shigenori; KITAGAWA, Teizo; FUKUZUMI, Shunichi[1]; ITOH, Shinobu[2]
([1]Osaka Univ.; [2]Osaka City Univ.)

[*J. Inorg. Biochem.* submitted (2003)]

Reactivity of the dicopper(I) and dicopper(II) complexes supported by novel polyamine ligands L1 (*N*,*N*'-dibenzyl-*N*-{3-[benzyl-(6-methyl-pyridin-2-ylmethyl)-amino]-propyl}-*N*'-(6-methyl-pyridin-2-ylmethyl)-propane-1,3-diamine) and L2 (*N*-benzyl-*N*-{2-[bis-(6-methyl-pyridin-2-ylmethyl)-amino]-ethyl}-*N*',*N*'-bis-(6-methyl-pyridin-2-ylmethyl)-ethane-1,2-diamine) towards O_2 and H_2O_2, respectively, have been investigated in order to shed light on the ligand effects on Cu_2/O_2 chemistry. The dicopper(I) complex of L1 (**1a**) readily reacted with O_2 in a 2 : 1 ratio at a low temperature (~ –90 °C) in acetone to afford a mixture of (μ-η^2:η^2-peroxo)dicopper(II) and bis(μ-oxo)dicopper(III) complexes. The formation of these two species has been confirmed by the ESR-silence of the solution as well as their characteristic absorption bands in the UV-vis region [λ_{max} = 350 and 510 nm due to the peroxo complex and ~ 400 nm due to the bis(μ-oxo) complex] and the resonance Raman bands at 729 cm^{-1} [$\Delta\nu(^{16}O_2\text{–}^{18}O_2)$ = 38 cm^{-1} due to the peroxo complex] and at 611 and 571 cm^{-1} [$\Delta\nu(^{16}O_2\text{–}^{18}O_2)$ = 22 cm^{-1} and 7 cm^{-1}, respectively, due to the bis(μ-oxo) complex]. The peroxo and bis(μ-oxo) complexes were unstable even at the low temperature, leading to oxidative *N*-dealkylation at the ligand framework. The dicopper(I) complex of L2 (**2a**) also reacted with O_2 to give (μ-hydroxo)-dicopper(II) complex ($\mathbf{2b^{OH}}$) as the product. In this case, however, no active oxygen intermediate was detected even at the low temperature (–94 °C). With respect to the copper(II) complexes, treatment of the (μ-hydroxo)dicopper(II) complex of L1 ($\mathbf{1b^{OH}}$) with an equimolar amount of H_2O_2 in acetone at –80 °C efficiently gave a (μ-1,1-hydroperoxo)dicopper(II) complex, the formation of which has been supported by its ESR-silence, UV-vis (370 and 650 nm) and resonance Raman spectra [881 cm^{-1}; $\Delta\nu(^{16}O_2\text{–}^{18}O_2)$ = 49 cm^{-1}]. The (μ-1,1-hydroperoxo)dicopper(II) intermediate of L1 also decomposed slowly at the low temperature to give similar oxidative *N*-dealkylation products. Kinetic studies on the oxidative *N*-dealkylation reactions have been performed to get insight into the reactivity of the active oxygen intermediates.